

Simultaneous EEG-fMRI Investigation of Rhythm-Dependent Thalamo-Cortical Circuits Alteration in Schizophrenia

Haonan Pei ^{*}, Sisi Jiang [†], Mei Liu [‡], Guofeng Ye [§], Yun Qin [¶] and Yayun Liu ^{||}

*The Clinical Hospital of Chengdu Brain Science Institute
MOE Key Lab for Neuroinformation, School of Life Science
and Technology, University of Electronic Science
and Technology of China, Chengdu, P. R. China*

^{*}haonan_pei@163.com

[†]jss_uestc@163.com

[‡]3037402795@qq.com


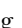
[§]18482020669@163.com

[¶]yunqin@uestc.edu.cn

^{||}756816322@qq.com

Mingjun Duan

*Department of Psychiatry, The Clinical Hospital of
Chengdu Brain Science Institute, University of Electronic
Science and Technology of China, Chengdu, P. R. China
fourhospital@163.com*

Dezhong Yao ^{**} and Cheng Luo ^{††}

*The Clinical Hospital of Chengdu Brain Science Institute
University of Electronic Science and Technology
of China, Chengdu 611731, P. R. China*

*High-Field Magnetic Resonance Brain Imaging Key Laboratory
of Sichuan Province, Center for Information in Medicine
University of Electronic Science and Technology of China, Chengdu, P. R. China*

*Research Unit of NeuroInformation Chinese
Academy of Medical Sciences, 2019RU035*

Chengdu, P. R. China

^{**}dyao@uestc.edu.cn

^{††}chengluo@uestc.edu.cn

Received 22 September 2023

Accepted 15 March 2024

Published Online 13 April 2024

Schizophrenia is accompanied by aberrant interactions of intrinsic brain networks. However, the modulatory effect of electroencephalography (EEG) rhythms on the functional connectivity (FC) in schizophrenia remains unclear. This study aims to provide new insight into network communication in schizophrenia by integrating

^{††} Corresponding author.

This is an Open Access article published by World Scientific Publishing Company. It is distributed under the terms of the [Creative Commons Attribution-NonCommercial 4.0 \(CC BY-NC\) License](https://creativecommons.org/licenses/by-nc/4.0/) which permits use, distribution and reproduction in any medium, provided that the original work is properly cited and is used for non-commercial purposes.

FC and EEG rhythm information. After collecting simultaneous resting-state EEG-functional magnetic resonance imaging data, the effect of rhythm modulations on FC was explored using what we term “dynamic rhythm information.” We also investigated the synergistic relationships among three networks under rhythm modulation conditions, where this relationship presents the coupling between two brain networks with other networks as the center by the rhythm modulation. This study found FC between the thalamus and cortical network regions was rhythm-specific. Further, the effects of the thalamus on the default mode network (DMN) and salience network (SN) were less similar under alpha rhythm modulation in schizophrenia patients than in controls ($mean\ ScZ : mean\ HC = 0.715 : 0.777$). However, the similarity between the effects of the central executive network (CEN) on the DMN and SN under gamma modulation was greater ($mean\ ScZ : mean\ HC = 0.695 : 0.629$), and the degree of coupling was negatively correlated with the duration of disease ($r = -0.373$, $p = 0.003$). Moreover, schizophrenia patients exhibited less coupling with the thalamus as the center and greater coupling with the CEN as the center. These results indicate that modulations in dynamic rhythms might contribute to the disordered functional interactions seen in schizophrenia.

Keywords: Simultaneous EEG-fMRI; adapted directed transfer function; physio-physiological interaction; rhythm dependence; schizophrenia.

1. Introduction

Schizophrenia is a chronic psychiatric disorder characterized by delusions, hallucinations, cognitive impairment^{1,2} and disordered communication among brain regions.^{3,4} Cognitive deficits have long been thought to be a central feature of schizophrenia.⁵ Recently, a number of studies looked at the relationship between deficits of network communication and symptom severity in schizophrenia. The unifying triple network model, proposed on the basis of functional magnetic resonance imaging (fMRI) data and consisting of salience network (SN), default mode network (DMN), and the central executive network (CEN), provides new insight into psychopathological and higher cognitive deficits.^{6–8} Numerous studies have reported that interactions within and between these neurocognitive networks are disrupted in schizophrenia,^{9–11} which may contribute to the positive symptoms of the disease.^{8,12} The thalamus is composed of multiple nuclei which are connected to the cortex and received the information.^{13–16} Recent works about seed-based thalamo-cortical connectivity revealed consistent patterns of hypoconnectivity between the thalamus and DMN and hyperconnectivity between the thalamus and sensorimotor network in schizophrenia.^{17,18} The thalamus is clearly involved in the pathological mechanisms of schizophrenia and might also play a role in working memory and attention deficits.^{15,16,19–21} Evidence suggests that the abnormal brain activity seen is likely caused by a breakdown in coordination among multiple networks in

schizophrenia. Thus, assessing network interactions might facilitate the understanding of the pathologic phenomenon of schizophrenia.

Brain rhythm information, which was extracted from electroencephalography (EEG), has been shown to be relevant to cognitive and physiological mechanisms of disease.^{22,23} Leicht *et al.* proved that a reduced activation of an auditory evoked gamma-band response-specific network in the high-risk state of psychosis subjects brought forward by EEG-informed fMRI.^{24–27} However, they only looked at rhythm-induced activity in brain regions and did not look at functional connections between brain regions. A recent study used the directed transfer function (DTF) to obtain information on five rhythms as characteristics, and subsequently used SVM to effectively distinguish patients with different states of schizophrenia.²⁸ They found that brain connectivity indices can be viewed as biomarkers for detecting schizotypal personality. But, temporal EEG information was not included in the analysis. Abnormalities in the thalamo-cortical circuit have been reported in several studies in schizophrenia.^{15,29,30} This circuit is thought to be related to the generation of alpha rhythms.³¹ Rhythm changes might reflect changes in interaction between brain regions within the circuit. Recent works have emphasized the effects of brain rhythms on functional connectivity (FC).^{32,33} But the relationship between brain rhythms and abnormal FC is not clear in patients. Simultaneous EEG-fMRI technique combines the advantages of high temporal resolution of EEG with

high spatial resolution of fMRI and allows localizing the blood oxygenation level-dependent (BOLD) correlates of spontaneous fluctuating features of the EEG.^{34,35} EEG and fMRI have been widely used to explore the pathological mechanisms of diseases, such as epilepsy.^{26,36–38} However, studies of schizophrenia lack such comprehensive analyses. Using simultaneous EEG-fMRI may aid exploration of the abnormalities seen in the relationship between rhythm and thalamo-cortical circuit in patients with schizophrenia.

In order to get a comprehensive picture of brain rhythm activity across the whole brain at different times, neuroimaging data were collected by simultaneous EEG-fMRI technique and we employed the adapted directed transfer function (ADTF) method, which, building upon DTF for extracting rhythmic relationships, also captures the temporal information of EEG.^{26,39,40} Furthermore, the physio-physiological interaction (PPI) model based on a general linear model, which is a neuroimaging method, is employed to investigate the dynamic interactions between different brain regions under identical rhythm modulation conditions.^{41,42} We also investigated coupling between multiple networks using multivariate distance correlation (MDC).⁴³ Our research framework characterized the synergistic functional relationships among any three cortical networks under identical rhythm modulation conditions, and we identified different coupling states of healthy controls (HC) and patients. By uncovering abnormal communication patterns that depend on rhythm information,

this study improves our understanding of the pathological features of schizophrenia and provides a novel analytical framework for exploring pathological changes.

2. Methods

2.1. Participants

All schizophrenia patients and HC were recruited from the Clinical Hospital of Chengdu Brain Science Institute of University of Electronic Science and Technology of China. The patients were diagnosed using the structured clinical interview for the DSM-V axis 1 disorders-clinical version (SCID-I-CV) from 2021 to 2022. No participants reported any neurological disorders, head injury, alcohol, or other substance abuse. The demographic and clinical information of all eligible participants is shown in Table 1. Legal guardian of patients and HC provided written informed consent and received monetary compensation. This study was approved by the ethical committee of the University of Electronic Science and Technology of China.

2.2. Data acquisition

We allocated 510 seconds of scanner time for simultaneous EEG and fMRI recording. Participants were instructed to keep their eyes closed, but to avoid falling asleep.

All participants were scanned on the 3T MR (Siemens, Skyra). Resting-state functional data were

Table 1. Demographic characteristics of patients with schizophrenia and controls.

	Patients	HC	<i>p</i> -value
Number	84	47	—
Age (years)	38.29 ± 12.87	45.40 ± 10.00	< 0.05 ^a
Gender (Male : Female)	14:70	12:35	0.222 ^b
Handedness (Right : Left)	84:0	47:0	NaN
Duration of illness (years)	9.02 ± 7.92	—	—
Chlorpromazine equivalents (mg/d) ^c	341.55 ± 158.31	—	—
PANSS-total ^d	77.43 ± 14.78	—	—
PANSS-positive ^d	19.97 ± 4.80	—	—
PANSS-negative ^d	23.81 ± 7.29	—	—
PANSS-general ^d	33.65 ± 5.55	—	—

Notes: ^a — Two-sample *t*-test; ^b — χ^2 test; ^c — Data of 67 patients available; ^d — PANSS scores of 74 patients with schizophrenia is available; PANSS — Positive and Negative Syndrome Scale.

obtained by using an echo-planar imaging sequence: TR = 2000 ms, TE = 30 ms, FA = 90°, matrix = 64 × 64, field of view = 24 × 24 cm², slices = 34, slice thickness = 4.4 mm, Spacing Between Slices = 4.4. Simultaneous EEG data were recorded using a 66-channel MR-compatible EEG cap (Neuroscan, Charlotte, NC) according to the 10–20 standard system of electrode placement with a reference at the Fcz position. The amplifier (Neuroscan, synAmps2) was placed outside the MR room, and the sampling rate was set at 5000 Hz. Electrode impedances were lowered to below 20 kΩ before recording. The EEG recording was synchronized with the MR scanner’s internal clock.

2.3. Preprocessing

All fMRI data were preprocessed using SPM12 and DPABI in MATLAB (MathWorks Inc).^{44,45} Briefly, after discarding the first five volumes, the remaining images were slice-time corrected, and spatially realigned to the first volume to reduce the effects of head motion and co-registered to a standardized EPI template in which the images were normalized to the Montreal Neurologic Institute (MNI) space and resampled to 3 × 3 × 3 mm³ voxels. Then functional images were spatially smoothed with a 6 mm full-width half maximum (FWHM) Gaussian kernel. In addition, regressing out the nuisance signals (including 24-parameter motion correction, the white matter and mean cerebrospinal fluid signals) and filtered (0.01–0.1 Hz) were performed. Nine people (eight schizophrenia patients and one HC) were excluded prior to analysis under the head motion criterion of 3 mm and 3°. Further, some brain areas of interest were selected, that is, cortical triple networks (DMN, SN, and CEN) and thalamus. Templates of cortical triple networks (DMN, SN, and CEN) and thalamus were defined in our published studies based on the independent component analysis.^{46,47} The Brainnetome template provides a publicly available brain parcellation template. If more than half of a brain region’s voxels are located within a specific network template, we define that brain region as a subregion of the corresponding network template. Therefore, a total of 39 brain regions in the cortex are included.⁴⁸ The thalamus was divided into eight subregions based on our previous proposed thalamus template, which also relied on the capability of the independent component analysis.⁴⁷

EEG data were preprocessed using the EEGLAB toolbox in MATLAB.⁴⁹ Firstly, MR gradient artifacts were removed by subtracting the averaged scanner artifact template from the continuous EEG recordings.⁵⁰ EEG recordings were band-pass filtered from 1 Hz to 45 Hz. The bad point was marked and deleted to clear the data by the clean_rawdata function of the EEGLAB toolbox (https://github.com/scn/clean_rawdata/wiki). The ballistocardiogram (BCG) artifacts were corrected using the optimal basis set.⁵¹ Blink artifacts and residual artifacts were removed using the independent component analysis method, and the preprocessed EEG was re-referenced to the neutral reference using the reference electrode standardization technique (REST).⁵² The data were further down-sampled to 100 Hz to reduce subsequent computational complexity and each point was matched to the single scan volume that corresponded to the collection time (1 TR = 2000 ms). For ease of calculation and analysis, N channels were selected ($N_{Channel} = 21$, FP1, FP2, FPZ, F7, F8, FZ, C3, C4, CZ, F3, F4, T7, T8, P7, P8, P3, P4, PZ, OZ, O1, O2).

2.4. Extracted time-varying information based on the ADTF

As described here,^{43,53,54} the connection matrix was constructed between preselected channels using ADTF.⁵⁵ The ADTF measure, which is based on multivariate adaptive autoregressive modeling (MVAR), is effective for delineating temporal changes in the connectivity strength and can also reveal the influence of a signal arising from one brain region on another region.⁵⁴ The MVAR was constructed by the following:

$$X_{EEG}(t) = \sum_{k=1}^p A(k, t) \cdot X_{EEG}(t - k) + E(t), \quad (1)$$

where p is the order of MVAR and can be determined by Bayesian information criterion, $X_{EEG}(t)$ is the data vector over time, $A(k, t)$ denotes the coefficient matrices of the time-varying model coefficients established by the Kalman filter algorithm⁵⁶ and $E(t)$ is multivariate independent white noise.

By transforming Eq. (1) into the frequency domain, we obtained

$$A(f, t) \cdot X_{EEG}(f, t) = E(f, t), \quad (2)$$

$$X_{\text{EEG}}(f, t) = A^{-1}(f, t) \cdot E(f, t), \quad (3)$$

where $A(f, t) = \sum_{k=0}^p A_k e^{-j2\pi f \Delta t k}$, $A_{k=0} = I$.

Therefore, the following equation is obtained:

$$X_{\text{EEG}}(f, t) = H(f, t) \cdot E(f, t), \quad (4)$$

The $H_{i,j}(f, t)$ is the transfer matrix of the system, which equals the inverse of frequency-transformed coefficient matrix.³⁹ Its elements, $H(f, t)$, represent the directional causal connection from the channel j to the channel i at time point t and frequency f . The normalized ADTF is described as follows:

$$\gamma_{ij}^2 = \frac{|H_{ij}(f, t)|^2}{\sum |H_i(f, t)|^2}, \quad \gamma_{ij}^2 \in (0, 1), \quad (5)$$

To evaluate total information flow from a given channel, ADTF values of individual frequency bands were summed. A value close to 1 indicates that most of the information in channel i is transferred from channel j .⁵³ A three-dimensional ADTF matrix ($N_{\text{Channel}} \times N_{\text{Channel}} \times T_e$, $T_e = 100 \times 500$ s) was obtained for each frequency band. Multiple frequency rhythms were analyzed to explore the information flow alteration, including delta (2–4 Hz), theta (4–8 Hz), alpha (8–12 Hz), beta (13–20 Hz), and gamma (30–45 Hz) rhythms.

The diagonal elements of the each ADTF matrix were removed. We calculated the mean and standard deviation of all elements on the time dimension and removed outliers (values > 4 standard deviations above or below the mean). After segmenting EEG data (200 timepoints/one segment/ $1TR$), we computed the proportion of viable time points, and subsequently removed data segments significantly impacted by artifacts (percentage threshold = 0.6). We summed the ADTF matrices after obtaining the average activity level for each 2-s segment. Thus, the dynamic rhythm information which consists of the mean of ADTF values was obtained.

2.5. Functional interactions between brain nodes under rhythm modulations

BOLD signals constitute an indirect measure of neural activity.⁵⁷ This study explored the question of whether functional interactions and information transmission among brain regions differ according to frequency rhythms using a PPI model based on a

general linear model.^{58,59} The PPI formula is

$$Y_{\text{ROI}_2} = \beta_0 + \beta_1 \cdot X_{\text{ROI}_1} + \beta_2 \cdot X_{\text{PI}} + \beta_3 \cdot (X_{\text{ROI}_1} \cdot X_{\text{PI}}) + \varepsilon, \quad (6)$$

where X_{ROI_1} and Y_{ROI_2} represent BOLD signals of two different ROIs. The β_3 value demonstrates how the contribution of one ROI (X_{ROI_1}) to another (Y_{ROI_2}) is altered by the physiological information (X_{PI}). The physiological information (X_{PI}) for a given frequency was obtained by convolving the dynamic rhythm information with the canonical hemodynamic response function. Then, an interactive connectivity matrix ($B_{ic} = N_{\text{ROI}} * N_{\text{ROI}}$) consisting of β_3 values is constructed for each subject. We conducted a normality test on the distribution of β_3 values, and under the threshold of $p < 0.05$, it conforms to a normal distribution. Differences between groups were examined using a two-sample t -test ($p < 0.05$), with age and sex as nuisance included covariates.

2.6. Functional coordination between brain networks depending on rhythm modulation

To further explore synergy among multiple networks in a given coupling pattern according to rhythm modulations, the MDC method was applied to determine the degree of coupling among three neurocognitive networks.⁶⁰ The MDC method is not affected by the number of ROIs in a brain network or the order of ROI storage in interactive connectivity matrices.⁶⁰ We divided the interactive connectivity matrix B_{ic} into submatrices, which stored values representing the influence of network BN_A on network BN_B . Four submatrices representing relationships between brain regions within the same network were excluded.

The first step is to compute the Euclidean distance between two interactive connectivity matrixes separately:

$$d1_{l,k} = \sqrt{\sum_{n=1}^{m_2} (B_{ic1_{ln}} - B_{ic1_{kn}})^2}, \quad l, k = 1, \dots, m_1, \quad (7)$$

$$d2_{l,k} = \sqrt{\sum_{n=1}^{m_3} (B_{ic2_{ln}} - B_{ic2_{kn}})^2}, \quad l, k = 1, \dots, m_1, \quad (8)$$

where submatrix B_{ic1} of m_1 by m_2 represents the contribution of BN_1 to BN_2 and submatrix B_{ic2} of m_1 by m_3 represents the contribution of BN_1 to BN_3 .

The U -centering is applied subsequently to ensure that row and column means are zero and that all expected values are zero:

$$P1_{l,k} = \begin{cases} D11 - D12 - D13 - D14, & l \neq k \\ 0, & l = k \end{cases}, \quad (9)$$

where $D11 = d1_{l,k}$, $D12 = \frac{1}{m_1-2} \sum_{j=1}^{m_1} d1_{l,j}$, $D13 = \frac{1}{m_1-2} \sum_{h=1}^{m_1} d1_{h,k}$, and $D14 = \frac{1}{(m_1-1)(m_1-2)} \sum_{j,h=1}^{m_1} d1_{h,j}$

By the same approach, we can get $P2_{l,k}$ using $d2_{l,k}$ by Eq. (9).

Finally, the MDC value is defined as

$$\text{dCor}(B_{ic1}, B_{ic2}) = \begin{cases} \sqrt{\frac{\text{dCov}(B_{ic1}, B_{ic2})}{\sqrt{\text{dVar}(B_{ic1}) \cdot \text{dVar}(B_{ic2})}}}, & \text{dCov}(B_{ic1}, B_{ic2}) > 0, \\ 0, & \text{dCov}(B_{ic1}, B_{ic2}) \leq 0, \end{cases} \quad (10)$$

where the dCov is distance covariance and the dVar is distance variance:

$$\text{dCov}(B_{ic1}, B_{ic2}) = \frac{1}{m_1(m_1-3)} \sum_{l,k=1}^{m_1} P1_{l,k} \cdot P2_{l,k}, \quad (11)$$

$$\text{dVar}(B_{ic1}) = \frac{1}{m_1(m_1-3)} \sum_{l,k=1}^{m_1} P1_{l,k}^2. \quad (12)$$

MDC shows the similarity between the effects of a given network (BN_1) on two other networks (BN_2 and BN_3). Thus, the MDC value represents the degree of coupling between BN_2 and BN_3 with BN_1 as an output center by the rhythm-modulation. When considering the similarity between the effects of two networks (BN_2 and BN_3) on another network (BN_1), the matrix representing the contribution of BN_2 to BN_1 (B_{ic1} ; m_2 by m_1) and the matrix representing the contribution of BN_3 to BN_1 (B_{ic2} ; m_3 by m_1) were used to calculate a new MDC value via the same steps described above. The new MDC value represents the degree of coupling between BN_2 and BN_3 with BN_1 as an input-center by the rhythm-modulation. According to previous studies,^{60,61} MDC values were converted to z -values by using Fisher's r -to- z transformation for subsequent

analysis. After conducting a normality test and observing data distributed within the range of 0–1, it was found that the data did not follow a normal distribution. Hence, the Wilcoxon rank sum test ($p < 0.05$) was adopted.

To explore the effects of the medicines taken by patients, we measured the drug dosage by chlorpromazine equivalents and calculated the correlation between chlorpromazine equivalents and the coupling degree.

2.7. Clustering analysis of multinetwork coupling

To identify strong and weak coupling under the same rhythm modulation conditions, the MDC values of all subjects in the HC group were connected in series to obtain the matrix of $N_{\text{Coup}} \times N_{\text{Sub}}$ (where N_{Coup} = the number of coupling combinations of networks, N_{Sub} = the number of healthy participants) and we applied a k -means clustering algorithm (for $k = 2$) using the square Euclidean distance.⁶² Initializations of cluster centroid positions were randomly selected 200 times (for $k = 2$) in MATLAB to obtain a stable solution. The clustering analysis aimed to maximize the distance between clusters and minimize the distance within clusters. Of the two clusters, one cluster showed a higher average degree of coupling than the other.

To determine the representative rhythm of each network coupling in the highly coupled cluster, a rhythm capable of maximizing the network coupling was assigned. In the lowly coupled cluster, the rhythm was assigned that can minimize the network coupling. This is seen as a representative rhythm of the corresponding coupling. On the basis of the clustering results, we compared alterations in the degree of coupling between the patient and HC groups. For validation, we also obtained results for three-cluster solutions ($k = 3$). In addition, we calculated correlations for clinical information using the Spearman correlation.

3. Results

3.1. ROI identification in four networks

In total, 47 ROIs (NROI) were selected, including 8 in the THA, 10 in the CEN, 13 in the SN and 16 in the DMN, as shown in Fig. 1.

3.2. Functional connections between nodes by rhythm modulations

The FC between brain regions modulated by rhythms indicated that there were both positive and negative internetwork relationships (Fig. 2). Further, we determined whether the dominant relationships between networks were rhythm-specific;

rhythm-specific and nonrhythm-specific “edges” are shown in the last two columns of each row in Fig. 2. The results regarding rhythm-modulated FC between brain regions are provided in the supplementary materials (Fig. A.1).

Neither group showed rhythm-specific effects of the THA on the SN, the THA on the CEN, or the

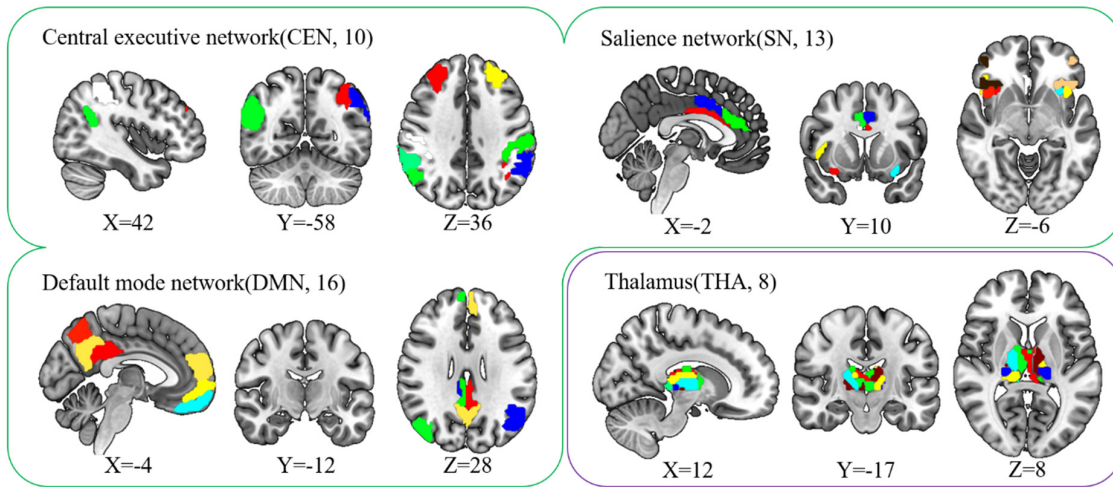


Fig. 1. ROIs presentation for four networks. Abbreviation: CEN, central executive network; DMN, default mode network; SN, salience network; THA, thalamus.

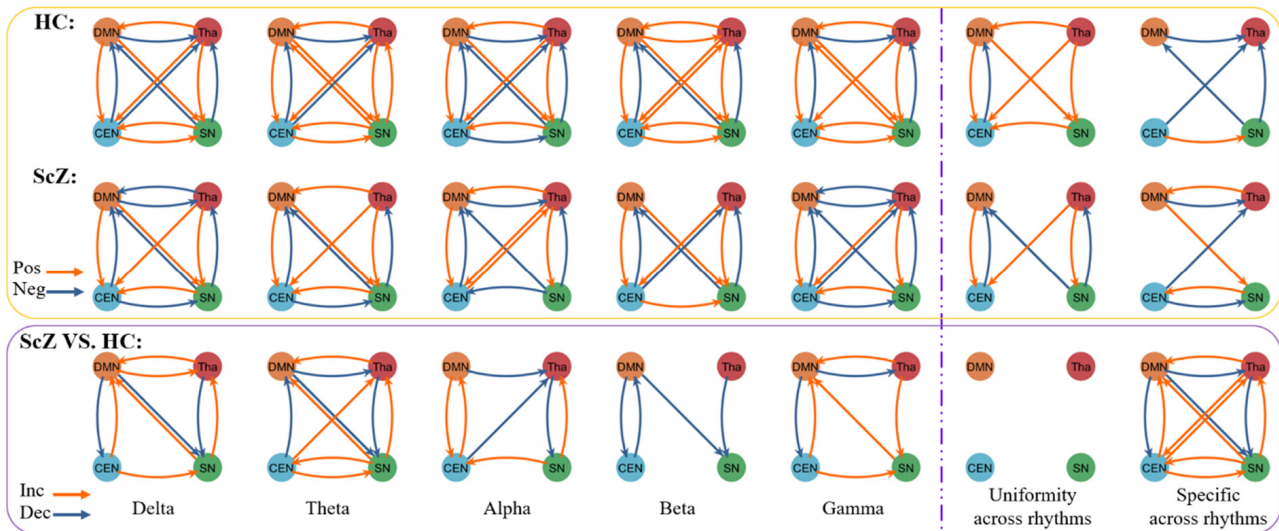


Fig. 2. Dominant trends and rhythm-specific effects in internetwork connectivity. The first two rows show dominant trends in internetwork connectivity of HC and ScZ, respectively. The third row shows the dominant trend of differences between the two groups. Corresponding intra-group uniform edges and specific edges across rhythm are shown in the last two columns of each row. The uniform edges across rhythm show the same dominant trend under different rhythm modulations, while the others show changes under different rhythm modulations. Abbreviation: Pos, positive connection; Neg, negative connection; Inc, increase connection; Dec, decrease connection.

DMN on the CEN. Unlike the HC group, the influence of the THA on the DMN, the DMN on the SN, and the SN on the CEN was not rhythm-specific in the schizophrenia group, although the effect of the SN on the DMN was rhythm-specific, as was that of the SN on the THA.

3.3. Functional coordination between brain networks affected by rhythms

The cluster states determined by k -means clustering algorithm ($k = 2$) in the HC are shown in Fig. 3. Thalamic-centered multinet network coupling was characterized by a higher degree of coupling than CEN-centered multinet network coupling. Similar results were obtained when the parameter $k = 3$ was selected, as shown in Fig. A.2.

Unlike CEN- and thalamic-centered coupling, rhythm-modulated DMN- and SN-centered coupling

did not behave consistently. The coupling between CEN and SN with DMN as a center by the rhythm-modulation was classified as the higher coupling cluster and the coupling between CEN and THA with DMN as the center was classified as the lower coupling cluster. The rhythm-modulated coupling between the SN and THA with DMN as the center was complex, being classified as lower-degree coupling under delta and gamma modulation and higher-degree coupling under alpha modulation. Moreover, the rhythm-modulated coupling between the CEN and DMN with SN as the center was classified as higher-degree coupling, whereas that between the CEN and THA with the SN as the center was classified as lower-degree coupling. Finally, the coupling between the CEN and THA with the SN as the center was classified as higher-degree coupling under alpha modulation and lower-degree coupling under delta and gamma modulation.

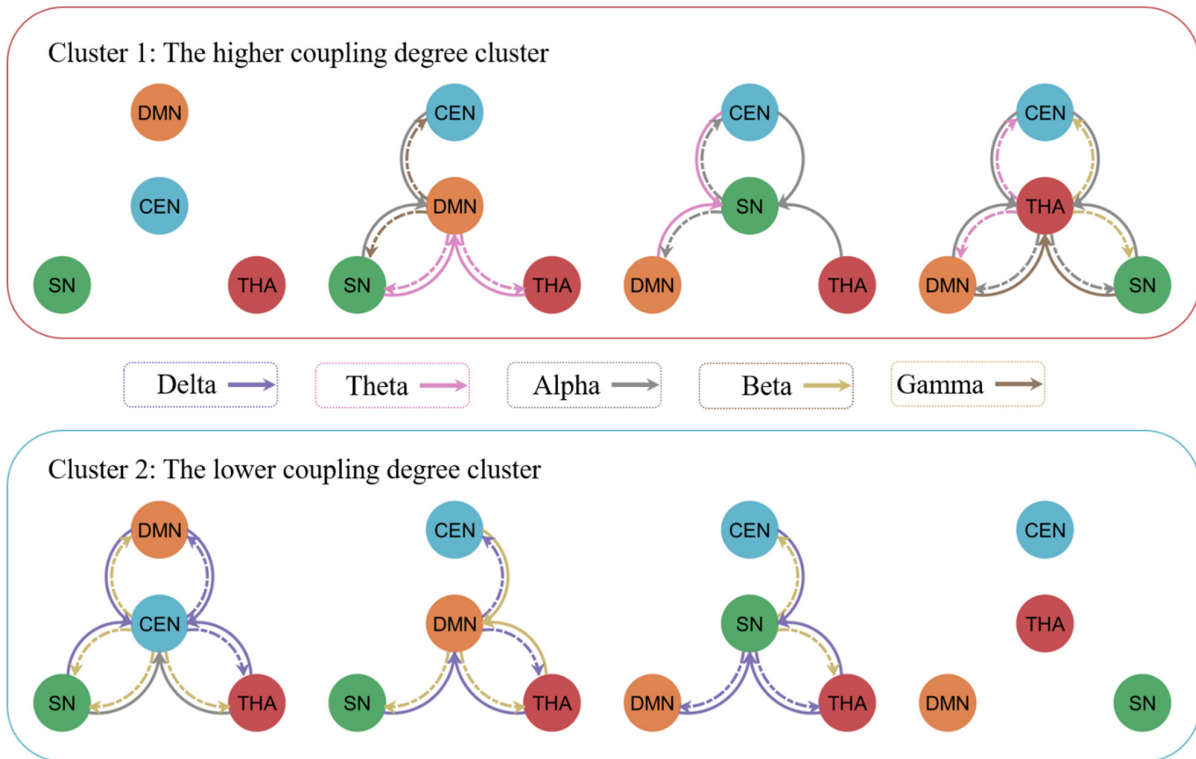


Fig. 3. Coupling relationship among multiple networks in two clusters (for $k = 2$). The arrow points to the affected area of the brain; different colors represent different rhythm, which indicate that the corresponding coupling relationship is present in this particular rhythm modulation; the dashed line represents the coupling degree between $BN2$ and $BN3$ with $BN1$ as an output-center by the rhythm-modulation, while the solid line represents the coupling degree between $BN2$ and $BN3$ with $BN1$ as an input-center by the rhythm-modulation. Abbreviation: M, mean; S, Standard deviation.

3.4. Alteration in the degree of coupling among brain networks under rhythm modulations

After the representative rhythm was assigned to the corresponding coupling, we further explored whether the patient's functional network coupling with

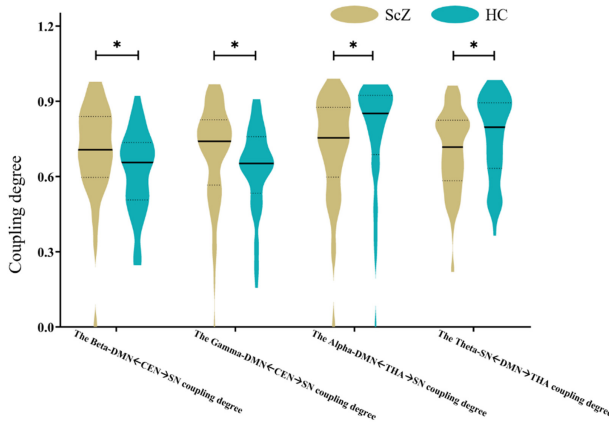


Fig. 4. Intergroup differences in coupling degree between multiple networks. Abbreviation: The “ $R-BN2 \leftarrow BN1 \rightarrow BN3$ ” coupling degree presents the coupling degree between $BN2$ and $BN3$ with $BN1$ as an output-center by the R -rhythm-modulation. For example, the Theta-SN←DMN→THA coupling presents the coupling degree between SN and thalamus with DMN as an output-center by the theta rhythm modulation. * — $p < 0.05$ (the Wilcoxon rank sum test).

representative rhythm modulation changes. As shown in Fig. 4, we found that the degree of coupling between the DMN and SN, with the CEN as the output center, was decreased under beta and gamma modulation. In contrast, the degree of coupling between the DMN and THA with the SN as the output center was increased under alpha modulation, as was the coupling between the SN and THA with the DMN as the output center under theta modulation.

We only found a correlation ($r = 0.294$, $p = 0.016$) between chlorpromazine equivalents and the coupling degree between DMN and SN with thalamus as an input-center by the gamma rhythm modulation. However, this coupling degree did not exhibit differences between the patient group and control group.

3.5. Correlation between coupling degree and clinical score

As shown in Fig. 5, the degree of coupling between the SN and THA, with the DMN as the output center, was significantly negatively correlated with the age of onset under theta modulation, and the coupling between the DMN and SN with the CEN as the output center was significantly negatively correlated with the duration of illness under gamma modulation.

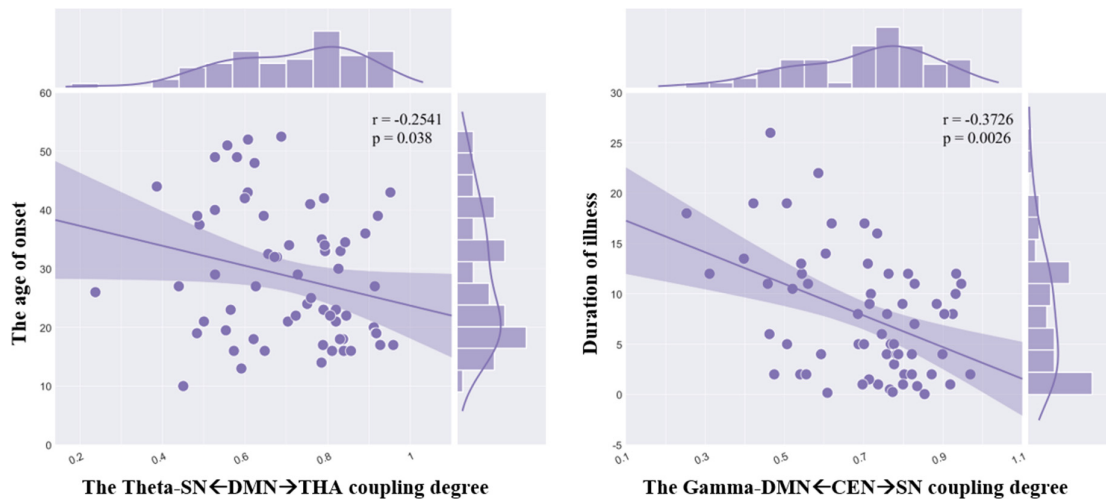


Fig. 5. Correlation between the coupling degree and clinical score. The Theta-SN←DMN→THA coupling presents the coupling degree between SN and thalamus with DMN as an output-center by the theta rhythm modulation; The Gamma-DMN←CEN→SN coupling presents the coupling degree between DMN and SN with CEN as an output-center by the theta rhythm modulation.

4. Discussion

Abnormal interactions between the thalamus and cortical triple networks in patients with schizophrenia were reported.^{15,63,64} In this study, we calculated the dynamic rhythm information and further explored rhythm-specific effects at the node and network levels using PPI based on simultaneous EEG-fMRI. We found that the influence of the thalamus on the DMN was identical among different dynamic rhythm information modulations, and the influence of the thalamus on the SN was rhythm-specific. In addition, we observed more complex connectivity alterations under low-frequency modulations involving the DMN, CEN, SN, and thalamus compared with high frequency modulations. Using MDC method, thalamus- and CEN-centered coupling were shown to be the strongest (coupling degree (Mean \pm Std) = 0.798 \pm 0.763) and weakest (coupling degree (Mean \pm Std) = 0.627 \pm 0.217) forms of coupling in HCs, respectively; the situation was reversed in schizophrenia patients. In particular, patients showed significantly decreased coupling among the DMN, SN, and thalamus under low-frequency oscillation modulations and stronger coupling among the DMN, SN, and CEN under high-frequency oscillations. Moreover, coupling between the DMN and SN, with the CEN as the center, was significantly negatively correlated with the duration of illness under gamma modulation. Taken together, our results suggest that the capacity of the thalamus to gate information is reduced, as is the ability of the CEN to regulate other networks, under dynamic rhythm information modulation in schizophrenia. These findings provide new insights into the neuro-pathological processes underlying schizophrenia.

4.1. Abnormal functional relationships between networks under low-frequency oscillation modulations

Coordinated neural activity depends on neural oscillations. Multiple studies have shown increased low-frequency activity in patients with schizophrenia.⁶⁵ Schizophrenia is characterized by reduced theta rhythm in frontal regions.⁶⁶ We found significant abnormalities in functional relationships modulated by low-frequency rhythms (delta and theta). The aberrant changes in patients with delta and theta modulation showed similar states, in which

functional relationships were concentrated in the functional connection between thalamus and DMN, thalamus and SN, CEN and DMN, and CEN and SN. There were no significant abnormal changes in the connections between the thalamus and CEN. It may be that abnormal interactions between the thalamus and the cortex of schizophrenia patients mainly involve connections with the DMN and SN, whereas for the CEN aberrant information exchange with the cortical network is more likely. Both delta and theta rhythms are related to cognitive function.^{27,67,68} We speculated that the processing and transmission of information in thalamus and the CEN were abnormal under low-frequency modulations, such that the DMN and SN would be unable to exchange information with the thalamus and CEN in a normal manner. This may lead to cognitive impairment in patients with schizophrenia. Neural oscillations may be crucial pathophysiological mechanisms in schizophrenia.^{66,69}

DMN is involved in several cognitive functions, such as self-reference, social cognition.⁷⁰ The inhibition of DMN and the switching of other network activity were dominated by a common mechanism. This mechanism had been reported in relation to SN activity.⁷⁰ We found the coupling between the thalamus and SN with the DMN as the center by theta modulation was decreased in schizophrenia and negatively correlated with the age of onset. It was further indicated that the interaction mechanism between DMN, SN and thalamus was problematic. Abnormal DMN activity by theta modulation may be associated with excessive self-reference and impairment in attention.⁷¹

4.2. Impaired interaction between thalamus and cortex

The thalamus is a diencephalic structure with primary functions including transmitting sensory information and helping to integrate cognitive processes.^{72,73} Abnormal structural and FC between the thalamus and cortical regions has been found in schizophrenia. In particular, our previous study revealed disturbed FC within cerebello-thalamo-cortical circuits.²⁹ In line with that study,⁷⁴ this study found abnormal connections of the thalamus with the DMN and SN. The influence (the positive dominant tendency) of the thalamus on DMN in

patients with schizophrenia was no longer altered by rhythm changes. Furthermore, although the positive dominant tendency of thalamic influence on SN is seen in HC, the influence of thalamus on SN was significantly decreased in schizophrenia, especially under the modulation of theta, alpha, and beta bands. Our results further indicated that abnormal relationships between the thalamus and DMN and SN were influenced by EEG rhythms.

In this study, we found a high degree of coupling between thalamus with cortical networks as a center in HC, implying similar relationships between the thalamus and various networks. This may be related to the role of thalamus in information transfer, where it is not “biased” against other network information processing. However, the degree of coupling between the DMN and SN with thalamus as a center was decreased in schizophrenia by alpha modulation. The alpha band reflects functional inhibition and alpha activity reduces the processing abilities of a given area.⁷⁵ The lower degree of coupling of patient may be caused by a failure of the alpha rhythm to regulate the network effectively. A relationship between the alpha rhythm and thalamic-cortical circuit has been proposed,^{31,76} and it may be dysregulated in schizophrenia. Danos *et al.* revealed significant positive correlations between alpha power and the rate of glucose metabolism in the thalamus in HCs but not in schizophrenia.³¹ We speculate that inadequate thalamic energy supply and alpha activity may be an important physiological mechanism in the dysregulation of the thalamic-cortical circuit. We found a decrease in thalamic-centered coupling involving cortical networks. Our results provide further evidence of a relationship between the alpha rhythm and the thalamic-cortical circuit. Dysfunction of the thalamus by alpha modulation might lead to failures of coordinating signals among various regions of the cortex. Converging evidence indicates that abnormalities of the thalamus and rhythms are highly important pathophysiology, which might be contributed to cognitive deficits.

4.3. Synergistic enhancement of multiple cortical networks

The dysregulation hypothesis was formulated following the development of neuroimaging methods, and

previous studies showed disruption of interactions within and among three neurocognitive networks in schizophrenia: CEN, DMN, and SN.^{9,10} It is necessary to study the connectivity among these brain networks because they play important roles in high-level cognition.^{77–79} Under beta and gamma band modulations, we found that the influence of the CEN on the DMN in patients with schizophrenia was predominantly negative, similar to what was seen in the HC group, although the influence of the CEN on the SN was in opposing directions between the two groups. Many studies investigating the association between the SN and CEN assumed a temporal lag in the relationship, and changes in direct FC were not apparent.⁸⁰ The results of this study indicate that the direct functional connection between the SN and CEN might be rhythm-specific; moreover, beta and gamma bands may be important in this respect.

At a broad level, the CEN supports the cognitive regulation of behavior, emotion, and thought,⁸¹ which requires attention to be directed toward pertinent stimuli.⁸² To achieve the required response flexibility, the CEN should regulate other networks in a specific manner. In this work, the low similarity of the interactions of multiple networks having the CEN as the center may reflect the specific regulatory role of the CEN. However, coupling was increased in schizophrenia patients, indicated especially by the significantly greater similarity of the effects of the CEN on the DMN and SN under beta rhythm modulation. Numerous studies have shown disrupted interactions between the CEN and DMN, and the CEN and SN, in schizophrenia.^{8,77,83} Our findings might provide further evidence that, under beta-band modulation, the CEN may be unable to influence different networks in a targeted way, resulting in a reduction in the ability of the CEN to maintain and manipulate information pertinent for problem-solving and decision-making.^{8,84}

Aberrant connections within the SN-CEN-DMN triple network have been demonstrated in schizophrenia, giving rise to positive symptoms.^{12,85} To more accurately determine the degree of coupling between the DMN and SN with the CEN as an output-center, we evaluated coupling under various rhythm modulations. Coupling was significantly stronger under gamma rhythm modulation in schizophrenia patients than HCs, and it was

negatively correlated with the duration of the disease. Gamma-band rendered communication precise and communication selective and provided a signature of cognitive state, as well as network dysfunction.^{86,87} This suggests that the modulation of functional connections by gamma rhythms also affects the selectivity of CEN to guide information from other networks. The effects of gamma rhythm modulation of the CEN on the SN and DMN in schizophrenia patients were similar (characterized by strong coupling) in the early stage of the disease but were clearly differentiated in disease of longer duration. We did not observe a significant correlation between changes in coupling and PANSS scale scores. We suggest that this may not strictly reflect functional normalization in brain networks, but rather a compensatory mechanism within DMN-CEN-SN circuits influencing the ability of the CEN to selectively regulate brain networks.

The degree of coupling between the DMN and SN, with the CEN as the output-center under the beta and gamma rhythm modulation, was significantly enhanced than HC, which might be explained by the beta and gamma bands being affected by disease progression and clinical symptoms.^{88,89} It has been suggested that abnormal beta rhythm in schizophrenia might be related to SN network dysfunction, while changes in gamma rhythm were found to be related to disease duration.⁸⁹ This implies that changes in coupling under beta and gamma rhythm modulations may be driven by different physiological mechanisms. The effects of the CEN on the SN and DMN may be regulated specifically by rhythm and may vary with disease duration. Moreover, the physiological mechanisms through which different rhythms modulate functional relationships between brain networks might be different. The abnormal changes seen in this study in schizophrenia patients affected the ability of the CEN to selectively integrate information.

The resting state of brain in schizophrenia is altered, as evidenced by changes in EEG and fMRI resting-state networks. Previous concurrent EEG-fMRI studies have tended to use general linear models to explore the brain states of patients, as it is a straightforward approach.⁹⁰⁻⁹² For example, Judith *et al.* found in their study that the N100 component is related to activation in the auditory cortex,

while Molly *et al.* discovered the correlation between load-dependent modulation of alpha suppression and BOLD signals in posterior parietal cortex.^{90,91} However, this pattern can only detect brain activity at the regions level or voxels level involved in rhythm, without describing the information exchange between brain regions or voxels. We incorporated the PPI model into the analysis framework, building upon the GLM, to additionally depict the interaction of information between different regions, providing further insight into the influence of rhythms on brain activity. Furthermore, Adamczyk *et al.* also employed simultaneous EEG-fMRI data to explore the states of patients with schizophrenia. In which, the effective connectivity was investigated using the DTF method, and they found the absence of increased source activity.⁹³ The DTF method delineates the effective connectivity between EEG electrodes; however, the results of DTF remove the superior temporal information inherent in EEG. Furthermore, the limitations of the DTF method render it challenging to directly integrate and analyze physiological activity recorded with fMRI. In this analysis framework, we utilize an improved version of the DTF method, termed ADTF, which, while retaining the ability to quantify the level of effective information transmission between electrodes, also preserves the high temporal resolution characteristics inherent in EEG. In the current work, we incorporate the additional temporal information provided by ADTF into the analysis, further increasing the feature dimensions in the multimodal fusion framework. This allows the fusion framework to provide more comprehensive and clear information for exploring brain states.

5. Limitations

Nonrhythm-specific connections merit further attention and exploration. These connections do not change as rhythms change, suggesting that they serve as the infrastructure for communication between brain networks. We speculate that these connections act as specialized conduits for different types of information. In this study, we did not explore the role of nonrhythm-specific edges alone. Exploring the consistency in functional coordination between, and rhythm specificity of, brain networks

might help us understand the basis of internetwork communication and the mechanisms underlying pathological changes.

Although we tried to ensure that the data collection and analysis processes were of high quality, the data may nevertheless have been influenced by machine and the degree of patient cooperation. More stringent data quality control methods are therefore needed. Moreover, MDC may not adequately describe the coupling or synergy between multiple networks.

In addition, the effects of drugs cannot be ignored. One study suggested that antipsychotics might partially remediate communication between the thalamus and cortex.⁶³ Hence, incomplete recovery of connections might be one of the reasons for the lower degree of coupling among networks with the thalamus as the center seen in this study. However, antipsychotic treatment as a variable was not included in our experimental design and the causal analysis was not performed. To explore the effects of antipsychotic treatment, more participants are needed, perhaps including first-diagnosed and drug-naive patients. There was no employment causality analysis method. To some extent, this prevents us from drawing conclusions. In future work, we plan to use causal analysis and longitudinal data to further explore the performance of patients with schizophrenia.

6. Conclusion

This study reported the effect of dynamic rhythm information on functional interactions between brain regions and functional coordination between brain networks in schizophrenia. We found that, under low-frequency oscillation modulations, patients with schizophrenia showed greater changes in FC involving the thalamus and three major cortical networks. Under rhythm modulations, the control group was

characterized by a high coupling mode with the thalamus as the center and a low coupling mode with the CEN as the center, whereas the reverse was seen in the schizophrenia patients. This suggests that, under dynamic rhythm information modulations, information exchange between the thalamus and cortical triple networks was dysfunctional, and the ability of the CEN to regulate other networks might therefore be weakened. These findings may reflect the pathological mechanisms underlying the abnormal connectivity patterns seen in patients with schizophrenia and provide new insights into the role of rhythms in those mechanisms.

Acknowledgments

This work was funded by a grant from the National Nature Science Foundation of China (Nos. 61933003, U2033217, 62201133 and 62003058), China Postdoctoral Science Foundation (No. 2021TQ0061), Chengdu Science and Technology Bureau (No. 2021-YF09-00107-SN), and the CAMS Innovation Fund for Medical Sciences (CIFMS) (No. 2019-I2M-5-039), Project of Science and Technology Department of Sichuan Province (Nos. 2022NSFSC1320 and 23NSFSC0016), the Fundamental Research Funds for the Central Universities (No. ZYGX2022 YGRH017).

The authors have no relevant financial or non-financial interests to disclose.

The data supporting the findings of this study are available from the corresponding author upon reasonable request.

The code supporting the findings of this study are available on the GitHub (<https://github.com/SchHNP/RDTCC>).

The Ethics Committee of the Clinical Hospital of Chengdu Brain Science Institute approved this study.

Appendix A

Table A.1. Regions of interest.

	Net	BA	Net	BA
NO01	CEN	IPL.L.6.2	NO25	DMN SFG.L.7.7
NO02	CEN	IPL.L.6.3	NO26	DMN SFG.R.7.7
NO03	CEN	IPL.L.6.4	NO27	SN CG.L.7.2
NO04	CEN	IPL.R.6.3	NO28	SN CG.L.7.3
NO05	CEN	IPL.R.6.4	NO29	SN CG.L.7.5
NO06	CEN	IPL.R.6.5	NO30	SN CG.R.7.2
NO07	CEN	MFG.L.7.1	NO31	SN CG.R.7.3
NO08	CEN	MFG.L.7.3	NO32	SN CG.R.7.5
NO09	CEN	MFG.L.7.4	NO33	SN IFG.R.6.5
NO10	CEN	MFG.R.7.1	NO34	SN INS.L.6.2
NO11	DMN	CG.L.7.1	NO35	SN INS.L.6.3
NO12	DMN	CG.R.7.1	NO36	SN INS.R.6.2
NO13	DMN	CG.R.7.4	NO37	SN INS.R.6.3
NO14	DMN	IPL.L.6.5	NO38	SN OrG.L.6.6
NO15	DMN	IPL.R.6.1	NO39	SN OrG.R.6.6
NO16	DMN	IPL.R.6.2	NO40	THA —
NO17	DMN	OrG.L.6.1	NO41	THA —
NO18	DMN	OrG.L.6.4	NO42	THA —
NO19	DMN	OrG.R.6.1	NO43	THA —
NO20	DMN	OrG.R.6.4	NO44	THA —
NO21	DMN	PCun.L.4.1	NO45	THA —
NO22	DMN	PCun.L.4.4	NO46	THA —
NO23	DMN	PCun.R.4.1	NO47	THA —
NO24	DMN	PCun.R.4.4		

Notes: The numbers on the left are used in Figs. 2 and A.1. Abbreviation: Net, Network; BA, Brainnetome Atlas; CEN, central executive network; DMN, default mode network; SN, salience network; IPL, Inferior parietal lobule; MFG, Middle Frontal Gyrus; CG, Cingulate Gyrus; IFG, Inferior Frontal Gyrus; INS, Insular Gyrus; OrG, Orbital Gyrus; PCun, Precuneus; SFG, Superior Frontal Gyrus.

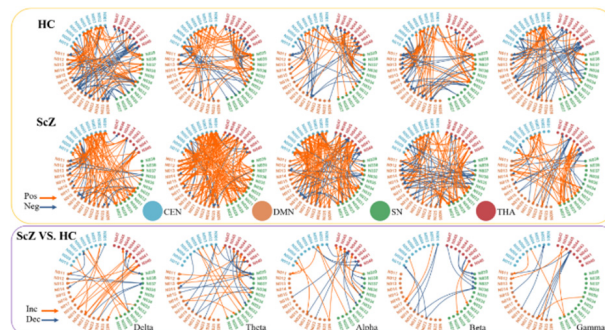


Fig. A.1. (Color online) The functional connections between brain regions changed under different rhythm modulations. The graphs in each column individually show functional connectivity changes modulated by delta, theta, alpha, beta, and gamma rhythms ($p < 0.05$, uncorrected). The orange box shows the results based on one-sample t -test and the purple box shows the results of inter-group comparison.

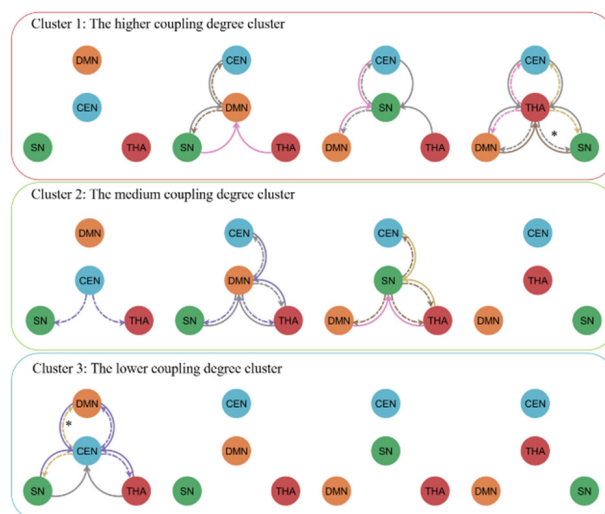










Fig. A.2. Coupling relationship among multiple networks in three clusters.

ORCID

Haonan Pei  <https://orcid.org/0000-0001-5202-5216>
 Sisi Jiang  <https://orcid.org/0000-0002-7430-9639>
 Mei Liu  <https://orcid.org/0009-0008-9227-7838>
 Guofeng Ye  <https://orcid.org/0009-0002-7179-4488>
 Yun Qin  <https://orcid.org/0000-0002-8106-6137>
 Yayun Liu  <https://orcid.org/0009-0001-9853-9199>
 Dezhong Yao  <https://orcid.org/0000-0002-8042-879X>
 Cheng Luo  <https://orcid.org/0000-0003-0524-5886>

References

1. M. J. Owen, A. Sawa and P. B. Mortensen, Schizophrenia, *Lancet (London, England)* **388**(10039) (2016) 86–97.
2. J. Richetto and U. Meyer, Epigenetic modifications in schizophrenia and related disorders: Molecular scars of environmental exposures and source of phenotypic variability, *Biol. Psychiatry* **89**(3) (2021) 215–226.
3. J. Fitzsimmons, M. Kubicki and M. E. Shenton, Review of functional and anatomical brain connectivity findings in schizophrenia, *Curr. Opin. Psychiatry* **26**(2) (2013) 172–187.
4. M. P. van den Heuvel and A. Fornito, Brain networks in schizophrenia, *Neuropsychol. Rev.* **24**(1) (2014) 32–48.
5. C. Dondé *et al.*, A century of sensory processing dysfunction in schizophrenia, *Eur. Psychiatry: J. Assoc. Eur. Psychiatrists* **59** (2019) 77–79.
6. D. Sridharan, D. J. Levitin and V. Menon, A critical role for the right fronto-insular cortex in switching between central-executive and default-mode networks, *Proc. Natl. Acad. Sci. USA* **105**(34) (2008) 12569–12574.
7. L. F. Barrett and A. B. Satpute, Large-scale brain networks in affective and social neuroscience: Towards an integrative functional architecture of the brain, *Curr. Opin. Neurobiol.* **23**(3) (2013) 361–372.
8. V. Menon, Large-scale brain networks and psychopathology: A unifying triple network model, *Trends Cogn. Sci.* **15**(10) (2011) 483–506.
9. S. Lefebvre *et al.*, Network dynamics during the different stages of hallucinations in schizophrenia, *Hum. Brain Mapp.* **37**(7) (2016) 2571–2586.
10. Q. Luo *et al.*, Effective connectivity of the right anterior insula in schizophrenia: The salience network and task-negative to task-positive transition, *NeuroImage Clin.* **28** (2020) 102377.
11. A. Manoliu *et al.*, Aberrant dependence of default mode/central executive network interactions on anterior insular salience network activity in schizophrenia, *Schizophr. Bull.* **40**(2) (2014) 428–437.
12. K. Supekar *et al.*, Dysregulated brain dynamics in a triple-network saliency model of schizophrenia and its relation to psychosis, *Biol. Psychiatry* **85**(1) (2019) 60–69.
13. A. S. Huang *et al.*, Characterizing effects of age, sex and psychosis symptoms on thalamocortical functional connectivity in youth, *NeuroImage* **243** (2021) 118562.
14. R. J. Piper *et al.*, Towards network-guided neuro-modulation for epilepsy, *Brain* **145**(10) (2022) 3347–3362.
15. P. Steullet, Thalamus-related anomalies as candidate mechanism-based biomarkers for psychosis, *Schizophr. Res.* **226** (2020) 147–157.
16. G. Pergola *et al.*, The role of the thalamus in schizophrenia from a neuroimaging perspective, *Neurosci. Biobehav. Rev.* **54** (2015) 57–75.
17. M. Giraldo-Chica and N. D. Woodward, Review of thalamocortical resting-state fMRI studies in schizophrenia, *Schizophr. Res.* **180** (2017) 58–63.
18. I. S. Ramsay, An activation likelihood estimate meta-analysis of thalamocortical dysconnectivity in psychosis, *Biol. Psychiatry Cogn. Neurosci. Neuroimaging* **4**(10) (2019) 859–869.
19. A. S. Huang, B. P. Rogers and N. D. Woodward, Disrupted modulation of thalamus activation and thalamocortical connectivity during dual task performance in schizophrenia, *Schizophr. Res.* **210** (2019) 270–277.
20. Z. Vukadinovic, NMDA receptor hypofunction and the thalamus in schizophrenia, *Physiol. Behav.* **131** (2014) 156–159.
21. N. D. Woodward, H. Karbasforoushan and S. Heckers, Thalamocortical dysconnectivity in schizophrenia, *Am. J. Psychiatry* **169**(10) (2012) 1092–1099.
22. R. Yuvaraj *et al.*, Brain functional connectivity patterns for emotional state classification in Parkinson's disease patients without dementia, *Behav Brain Res.* **298**(Pt B) (2016) 248–260.
23. M. Ahmadi and H. Adeli, Complexity of weighted graph: A new technique to investigate structural complexity of brain activities with applications to aging and autism, *Neurosci. Lett.* **650** (2017) 103–108.
24. G. Leicht *et al.*, EEG-informed fMRI reveals a disturbed gamma-band-specific network in subjects at high risk for psychosis, *Schizophr. Bull.* **42**(1) (2016) 239–249.
25. M. Ahmadi, H. Adeli and A. Adeli, Spatiotemporal analysis of relative convergence of EEGs reveals

- differences between brain dynamics of depressive women and men, *Clin EEG Neurosci.* **44**(3) (2013) 175–181.
26. U. R. Acharya et al., Computer-aided diagnosis of depression using EEG signals, *Eur. Neurol.* **73**(5–6) (2015) 329–336.
 27. M. Ahmadlou et al., Complexity of functional connectivity networks in mild cognitive impairment subjects during a working memory task, *Clin. Neurophysiol.* **125**(4) (2014) 694–702.
 28. A. Zandbagleh et al., Classification of low and high schizotypy levels via evaluation of brain connectivity, *Int. J. Neural Syst.* **32**(4) (2022) 2250013.
 29. J. Gong et al., Evaluation of functional connectivity in subdivisions of the thalamus in schizophrenia, *Br. J. Psychiatry* **214**(5) (2019) 288–296.
 30. J. A. Bernard, J. M. Orr and V. A. Mittal, Cerebello-thalamo-cortical networks predict positive symptom progression in individuals at ultra-high risk for psychosis, *NeuroImageClin.* **14** (2017) 622–628.
 31. P. Danos et al., EEG alpha rhythm and glucose metabolic rate in the thalamus in schizophrenia, *Neuropsychobiology* **43**(4) (2001) 265–272.
 32. J. Wirsich, A. L. Giraud and S. Sadaghiani, Concurrent EEG- and fMRI-derived functional connectomes exhibit linked dynamics, *NeuroImage* **219** (2020) 116998.
 33. M. Nentwich et al., Functional connectivity of EEG is subject-specific, associated with phenotype, and different from fMRI, *NeuroImage* **218** (2020) 117001.
 34. Y. Qin et al., BOLD-fMRI activity informed by network variation of scalp EEG in juvenile myoclonic epilepsy, *NeuroImage Clin.* **22** (2019) 101759.
 35. S. Zhang et al., Multi-view graph contrastive learning via adaptive channel optimization for depression detection in EEG signals, *Int. J. Neural Syst.* **33**(11) (2023) 2350055.
 36. L. Zhang et al., Adolescent depression detection model based on multimodal data of interview audio and text, *Int. J. Neural Syst.* **32**(11) (2022) 2250045.
 37. U. R. Acharya et al., Automated EEG-based screening of depression using deep convolutional neural network, *Comput. Methods Programs Biomed.* **161** (2018) 103–113.
 38. A. Broutian et al., Bitemporal independent 3-Hz spike-and-waves in adult patient with idiopathic generalized epilepsy and Graves disease, *Clin. Neurophysiol. Pract.* **5** (2020) 206–208.
 39. C. Wilke, L. Ding and B. He, Estimation of time-varying connectivity patterns through the use of an adaptive directed transfer function, *IEEE Trans. Biomed. Eng.* **55**(11) (2008) 2557–2564.
 40. M. Ahmadlou, H. Adeli and A. Adeli, Fractality analysis of frontal brain in major depressive disorder, *Int. J. Psychophysiol.* **85**(2) (2012) 206–211.
 41. H. Fukuda et al., Computing social value conversion in the human brain, *J. Neurosci.* **39**(26) (2019) 5153–5172.
 42. P. Toivainen et al., The chronnectome of musical beat, *NeuroImage* **216** (2020) 116191.
 43. Y. Qin et al., Rhythmic network modulation to thalamocortical couplings in epilepsy, *Int. J. Neural Syst.* **30**(11) (2020) 2050014–2050014.
 44. J. Ashburner, SPM: A history, *NeuroImage* **62**(2) (2012) 791–800.
 45. C.-G. Yan et al., DPABI: Data processing & analysis for (resting-state) brain imaging, *Neuroinformatics* **14**(3) (2016) 339–351.
 46. H. He et al., Reduction in gray matter of cerebellum in schizophrenia and its influence on static and dynamic connectivity, *Hum. Brain Mapp.* **40**(2) (2019) 517–528.
 47. S. Jiang et al., Aberrant thalamocortical connectivity in juvenile myoclonic epilepsy, *Int. J. Neural Syst.* **28**(1) (2018) 1750034.
 48. L. Fan et al., The human brainnetome atlas: A new brain atlas based on connectional architecture, *Cereb. Cortex (New York)* **26**(8) (2016) 3508–3526.
 49. A. Delorme and S. Makeig, EEGLAB: An open source toolbox for analysis of single-trial EEG dynamics including independent component analysis, *J. Neurosci. Methods* **134**(1) (2004) 9–21.
 50. R. K. Niazy et al., Removal of FMRI environment artifacts from EEG data using optimal basis sets, *NeuroImage* **28**(3) (2005) 720–737.
 51. Y. Leclercq et al., fMRI artefact rejection and sleep scoring toolbox, *Comput. Intell. Neurosci.* **2011** (2011) 598206.
 52. D. Yao, A method to standardize a reference of scalp EEG recordings to a point at infinity, *Physiol. Meas.* **22**(4) (2001) 693–711.
 53. P. van Mierlo et al., Accurate epileptogenic focus localization through time-variant functional connectivity analysis of intracranial electroencephalographic signals, *NeuroImage* **56**(3) (2011) 1122–1133.
 54. S. F. Storti et al., Exploring the epileptic brain network using time-variant effective connectivity and graph theory, *IEEE J. Biomed. Health Inf.* **21**(5) (2017) 1411–1421.
 55. B. He et al., eConnectome: A MATLAB toolbox for mapping and imaging of brain functional connectivity, *J. Neurosci. Methods* **195**(2) (2011) 261–269.
 56. M. Arnold et al., Adaptive AR modeling of nonstationary time series by means of Kalman filtering, *IEEE Trans. Biomed. Eng.* **45**(5) (1998) 553–562.
 57. N. K. Logothetis and B. A. Wandell, Interpreting the BOLD signal, *Annu. Rev. Physiol.* **66** (2004) 735–769.
 58. K. J. Friston et al., Psychophysiological and modulatory interactions in neuroimaging, *NeuroImage* **6**(3) (1997) 218–229.

59. A. S. Greene *et al.*, How tasks change whole-brain functional organization to reveal brain-phenotype relationships, *Cell Rep.* **32**(8) (2020) 108066.
60. L. Geerligs, C. Cam and R. N. Henson, Functional connectivity and structural covariance between regions of interest can be measured more accurately using multivariate distance correlation, *NeuroImage* **135** (2016) 16–31.
61. Z. Lu *et al.*, Abnormal intra-network architecture in extra-striate cortices in amblyopia: A resting state fMRI study, *Eye Vision (London, England)* **6** (2019) 20.
62. S. Lloyd, Least squares quantization in PCM, *IEEE Trans. Inf. Theory* **28**(2) (1982) 129–137.
63. S. Chopra *et al.*, Functional connectivity in antipsychotic-treated and antipsychotic-naive patients with first-episode psychosis and low risk of self-harm or aggression: A secondary analysis of a randomized clinical trial, *JAMA Psychiatry* **78**(9) (2021) 994–1004.
64. W.-S. Kim *et al.*, Altered thalamic subregion functional networks in patients with treatment-resistant schizophrenia, *World J. Psychiatry* **12** (2022) 693–707, doi: 10.5498/wjp.v12.i5.693.
65. N. N. Boutros *et al.*, The status of spectral EEG abnormality as a diagnostic test for schizophrenia, *Schizophr. Res.* **99**(1–3) (2008) 225–237.
66. P. J. Uhlhaas and W. Singer, Abnormal neural oscillations and synchrony in schizophrenia, *Nat. Rev. Neurosci.* **11**(2) (2010) 100–113.
67. B. Güntekin and E. Başar, Review of evoked and event-related delta responses in the human brain, *Int. J. Psychophysiol.* **103** (2016) 43–52.
68. W. Klimesch, EEG alpha and theta oscillations reflect cognitive and memory performance: A review and analysis, *Brain Res. Rev.* **29**(2–3) (1999) 169–195.
69. U. R. Acharya *et al.*, A novel depression diagnosis index using nonlinear features in EEG signals, *Eur. Neurol.* **74**(1–2) (2015) 79–83.
70. V. Menon, 20 years of the default mode network: A review and synthesis, *Neuron* **111**(16) (2023) 2469–2487.
71. S. Whitfield-Gabrieli and J. M. Ford, Default mode network activity and connectivity in psychopathology, *Annu. Rev. Clin. Psychol.* **8** (2012) 49–76.
72. M. Perez-Rando *et al.*, Alterations in the volume of thalamic nuclei in patients with schizophrenia and persistent auditory hallucinations, *NeuroImage Clin.* **35** (2022) 103070.
73. M. Wolff and S. D. Vann, The cognitive thalamus as a gateway to mental representations, *J. Neurosci.: Off. J. Soc. Neurosci.* **39**(1) (2019) 3–14.
74. I. S. Ramsay *et al.*, Thalamocortical connectivity and its relationship with symptoms and cognition across the psychosis continuum, *Psychol. Med.* **53**(12) (2023) 5582–5591.
75. O. Jensen and A. Mazaheri, Shaping functional architecture by oscillatory alpha activity: Gating by inhibition, *Front. Hum. Neurosci.* **4** (2010) 186.
76. F. M. Howells *et al.*, Electroencephalographic delta/alpha frequency activity differentiates psychotic disorders: A study of schizophrenia, bipolar disorder and methamphetamine-induced psychotic disorder, *Transl. Psychiatry* **8** (2018) 75, doi: 10.1038/s41398-018-0105-y.
77. Y.-B. Xi *et al.*, Triple network hypothesis-related disrupted connections in schizophrenia: A spectral dynamic causal modeling analysis with functional magnetic resonance imaging, *Schizophr. Res.* **233** (2021) 89–96.
78. S. Y. Chan *et al.*, Impact of substance use disorder on between-network brain connectivity in early psychosis, *Schizophr. Bull. Open* **3**(1) (2022) sgac014.
79. B. Garcia-Martinez *et al.*, Evaluation of brain functional connectivity from electroencephalographic signals under different emotional states, *Int. J. Neural Syst.* **32**(10) (2022) 2250026.
80. Q. Chen *et al.*, Aberrant structural and functional connectivity in the salience network and central executive network circuit in schizophrenia, *Neurosci. Lett.* **627** (2016) 178–184.
81. G. E. Miller *et al.*, Functional connectivity in central executive network protects youth against cardiometabolic risks linked with neighborhood violence, *Proc. Natl. Acad. Sci. USA* **115**(47) (2018) 12063–12068.
82. W. W. Seeley *et al.*, Dissociable intrinsic connectivity networks for salience processing and executive control, *J. Neurosci.: Off. J. Soc. Neurosci.* **27**(9) (2007) 2349–2356.
83. W. Han *et al.*, Low-rank network signatures in the triple network separate schizophrenia and major depressive disorder, *NeuroImage Clin.* **22** (2019) 101725.
84. A. Manoliu *et al.*, Insular dysfunction reflects altered between-network connectivity and severity of negative symptoms in schizophrenia during psychotic remission. *Front. Hum. Neurosci.* **7** (2013) 216.
85. Y. Jiang *et al.*, Common and distinct dysfunctional patterns contribute to triple network model in schizophrenia and depression: A preliminary study, *Progr. Neuro-psychopharmacol. Biol. Psychiatry* **79** (Pt B) (2017) 302–310.
86. P. Fries, Rhythms for cognition: Communication through coherence, *Neuron* **88**(1) (2015) 220–235.
87. X. Jia and A. Kohn, Gamma rhythms in the brain, *PLoS Biol.* **9**(4) (2011) e1001045.
88. M. Maran, T. Grent-‘t-Jong and P. J. Uhlhaas, Electrophysiological insights into connectivity anomalies in schizophrenia: A systematic review, *Neuropsychiatric Electrophysiol.* **2**(1) (2016) 6.
89. G. Di Lorenzo *et al.*, Altered resting-state EEG source functional connectivity in schizophrenia: The

- effect of illness duration, *Front. Hum. Neurosci.* **9** (2015) 234.
90. J. M. Ford et al., Using concurrent EEG and fMRI to probe the state of the brain in schizophrenia, *Neuro-Image Clin.* **12** (2016) 429–441, doi: 10.1016/j.nicl.2016.08.009.
91. M. A. Erickson et al., Neural basis of the visual working memory deficit in schizophrenia: Merging evidence from fMRI and EEG, *Schizophr. Res.* **236** (2021) 61–68.
92. S. M. Gorka, K. L. Phan and S. A. Shankman, Convergence of EEG and fMRI measures of reward anticipation, *Biol. Psychol.* **112** (2015) 12–19.
93. P. Adamczyk et al., On the role of bilateral brain hypofunction and abnormal lateralization of cortical information flow as neural underpinnings of conventional metaphor processing impairment in schizophrenia: An fMRI and EEG study, *Brain Topogr.* **34**(4) (2021) 537–554.